计算视觉与模式识别

黑体辐射

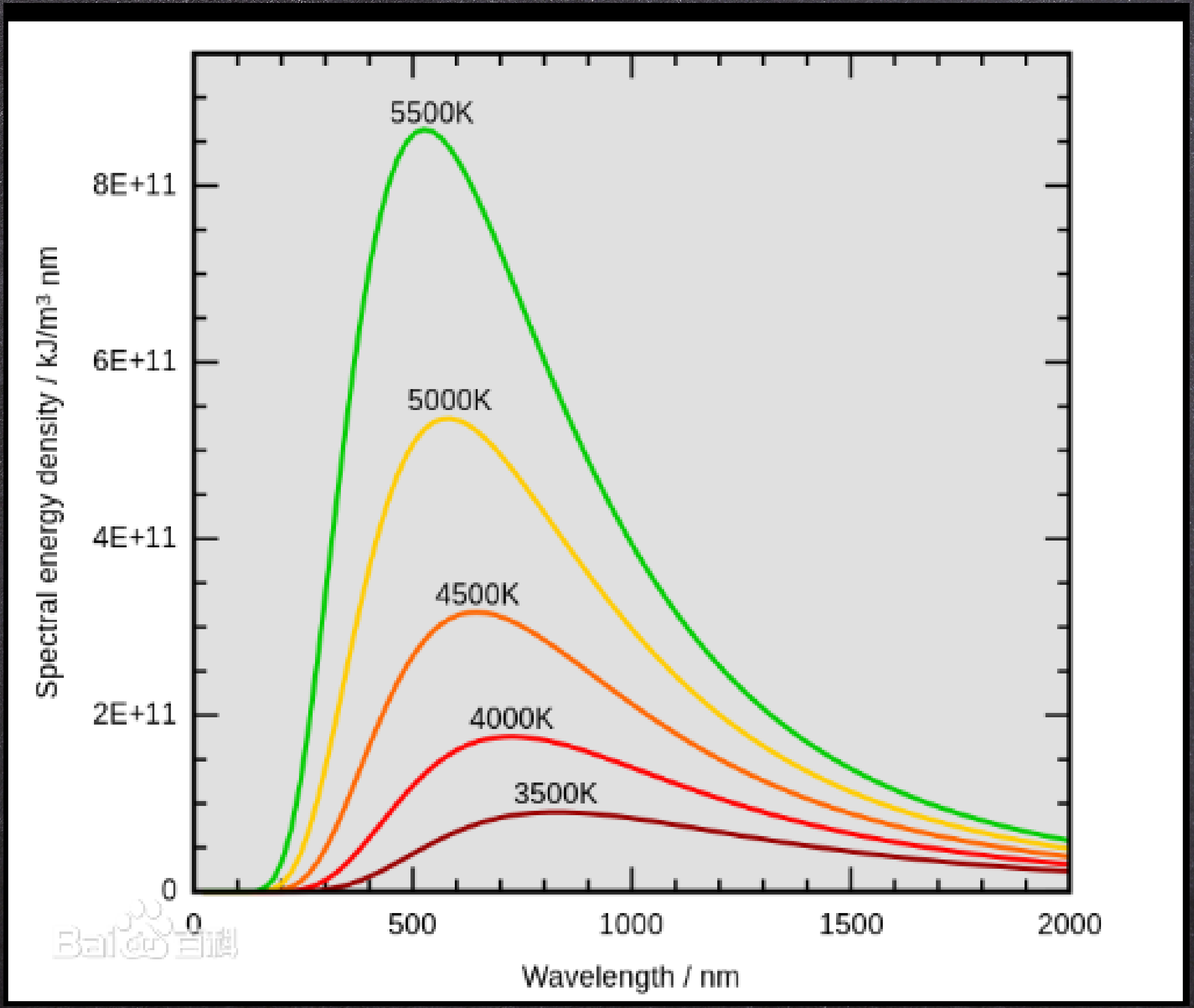
5500K
5000K
4500K
4000K
3500K
8E+11
6E+11
4E+11
2E+11
0
0
500
1000
1500
2000
Spectral energy density / kJ/m³ nm
Wavelength / nm
Bai百科

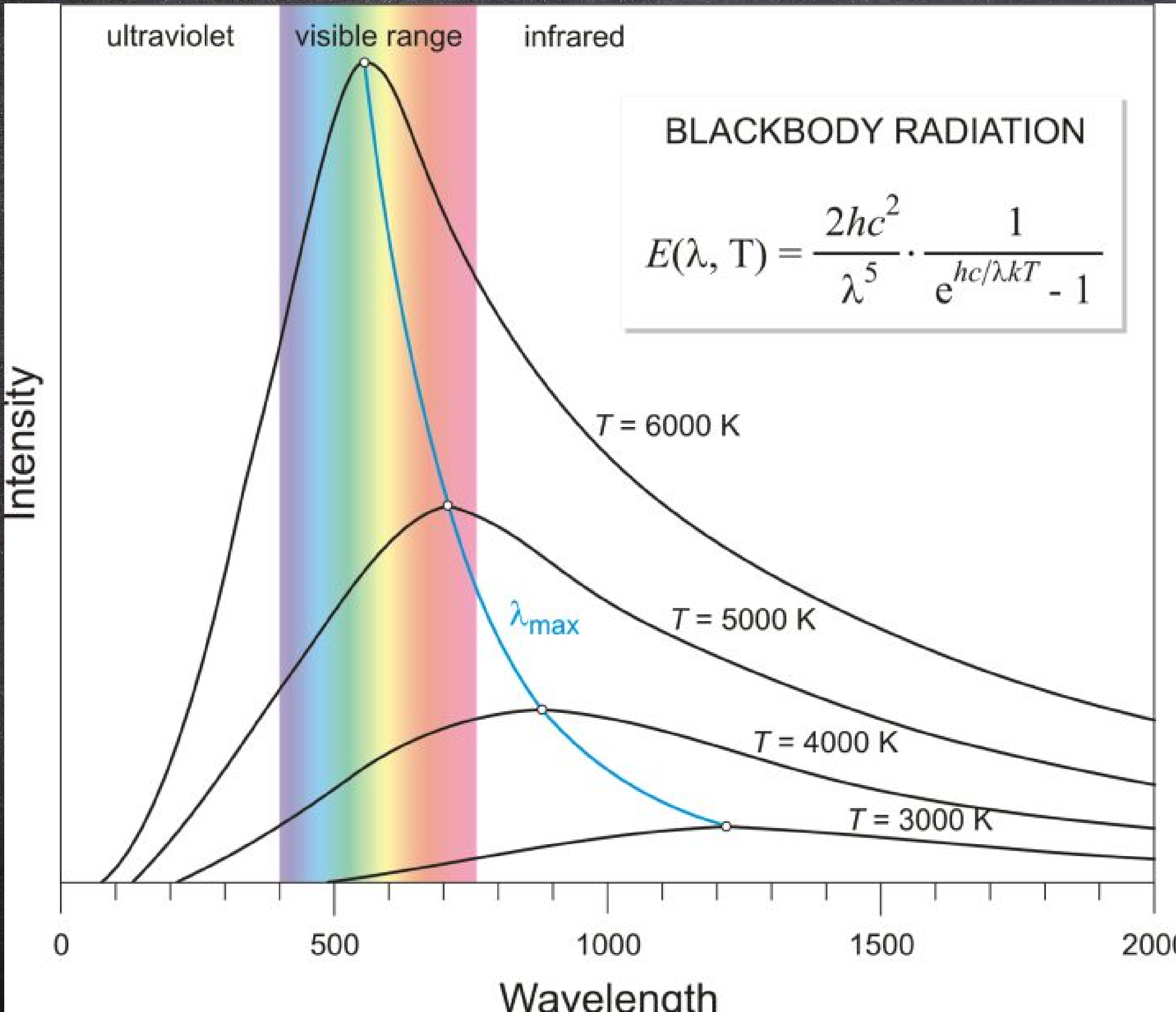

ultraviolet
visible range
infrared
BLACKBODY RADIATION
$$E(\lambda, T) = \frac{2hc^2}{\lambda^5} \cdot \frac{1}{e^{hc/\lambda kT} - 1}$$
T = 6000 K
T = 5000 K
T = 4000 K
T = 3000 K
λ_{max}
Intensity
0
500
1000
1500
2000
Wavelength

太阳与天空

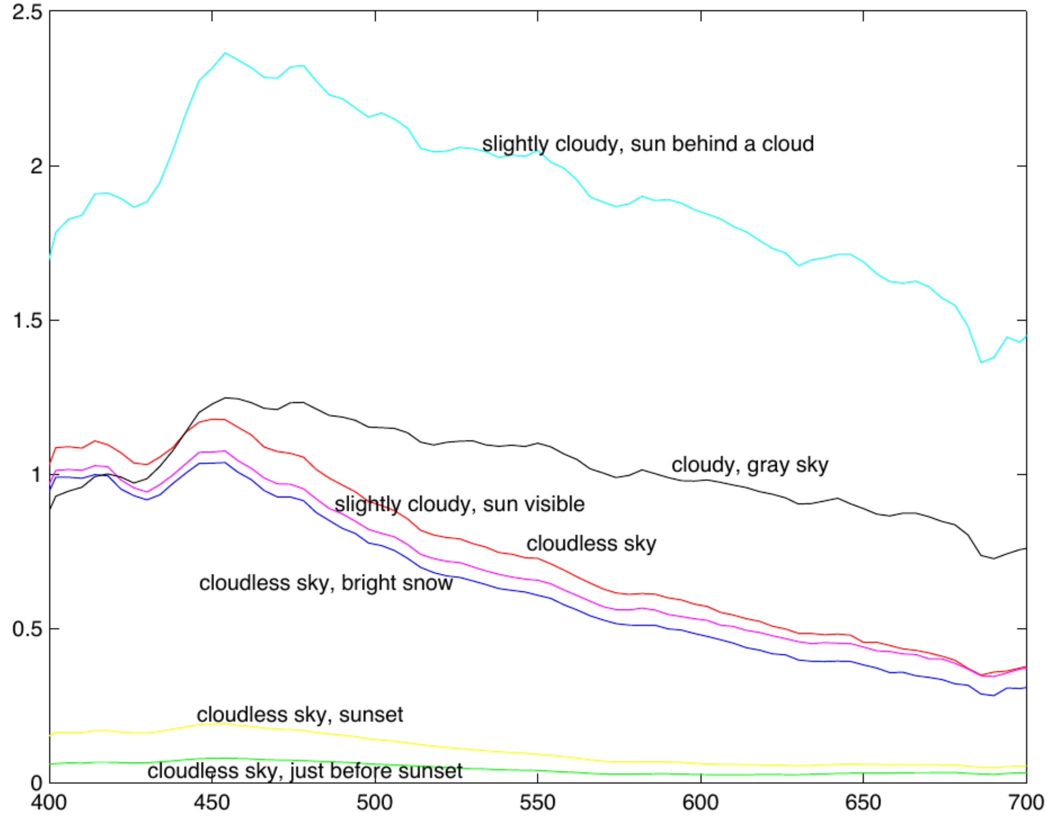

Figure 4.3. There are significant variations in the relative spectral power of daylight measured at different times of day and under different conditions. The figure shows a series of seven different daylight measurements, made by Jussi Parkkinen and Pertti Silfsten, of daylight illuminating a sample of barium sulphate (which gives a very high reflectance white surface). Plot from data obtainable at `http://www.it.lut.fi/research/color/lutcs_database.html`.

灯光

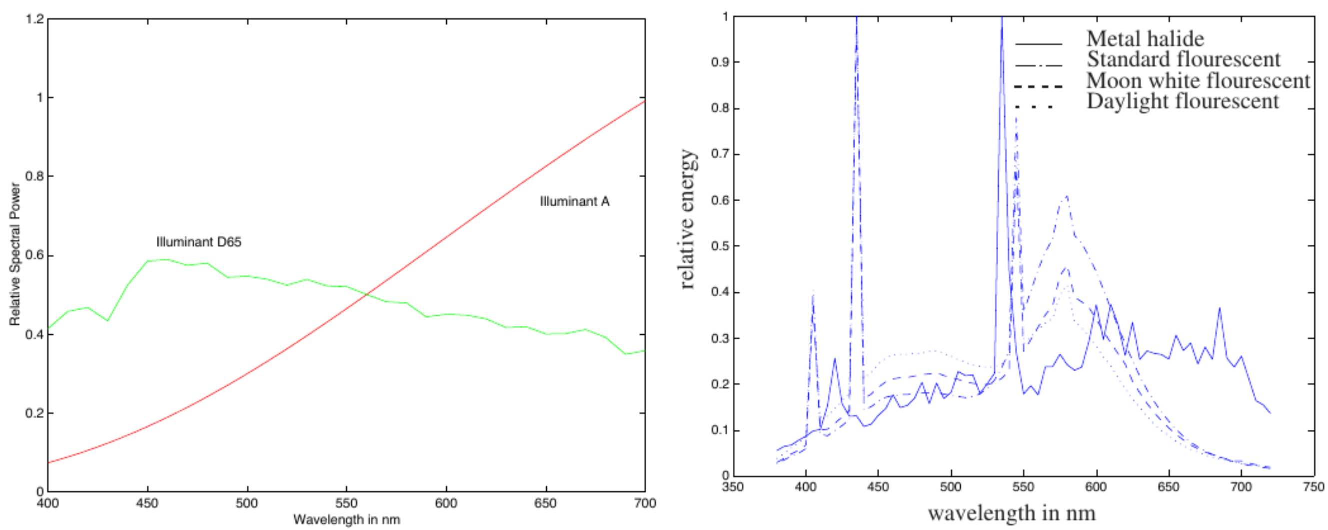

Figure 4.4. There is a variety of illuminant models; the graph shows the relative spectral power distribution of two standard CIE models, illuminant A — which models the light from a 100W Tungsten filament light bulb, with colour temperature 2800K — and illuminant D-65 — which models daylight. *Figure plotted from data available at* `http://www-cvrl.ucsd.edu/index.htm`.The relative spectral power distribution of four different lamps from the Mitsubishi Electric corp, measured by ****, data from *****. Note the bright, narrow bands that come from the flourescing phosphors in the fluorescent lamp.

表面的颜色

朗伯加镜面反射模型：

$$E(\lambda) \;=\; \rho_{\mathrm{dh}}(\lambda)S(\lambda)\times \text{geometric terms}+\text{specular terms}$$

光谱反射率——花与叶

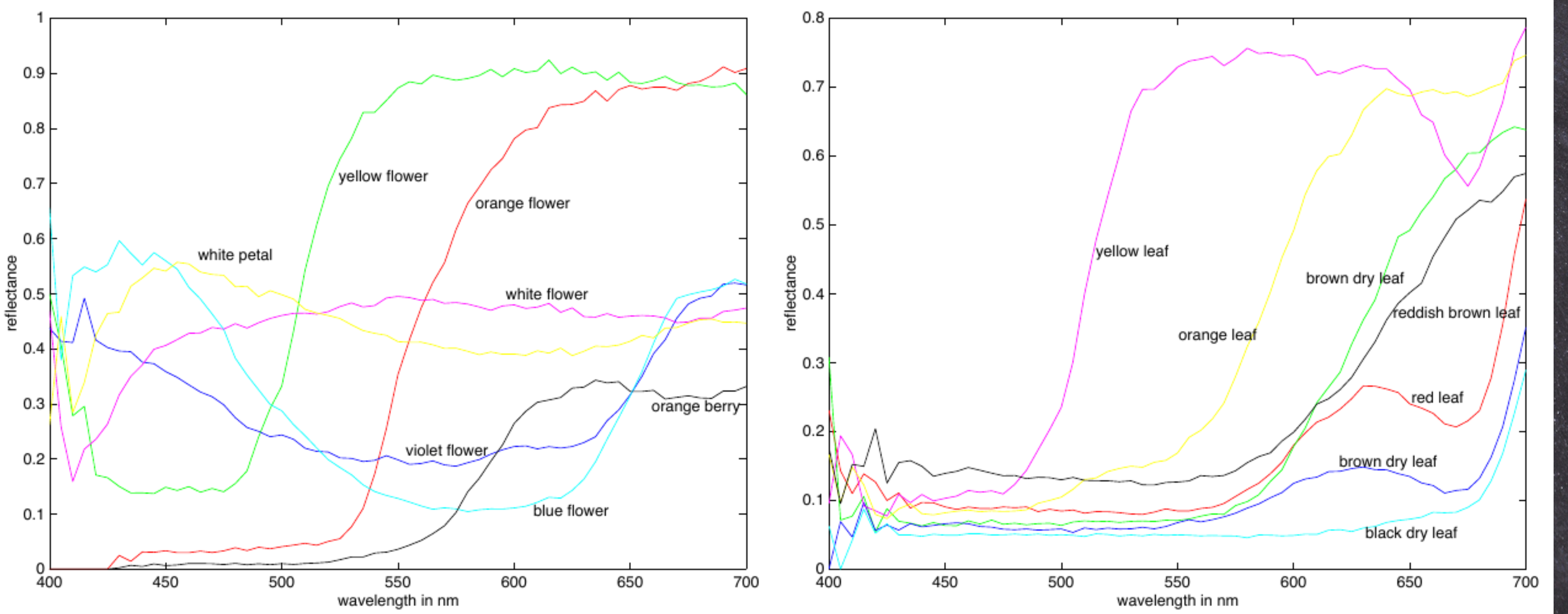

Figure 4.1. Spectral albedoes for a variety of natural surfaces, measured by Esa Koivisto, Department of Physics, University of Kuopio, Finland. On the left, albedoes for a series of different natural surfaces — a colour name is given for each. On the right, albedoes for different colours of leaf; again, a colour name is given for each. These figures were plotted from data available at `http://www.it.lut.fi/research/color/lutcs_database.html`.

光谱反射率——红花与绿叶

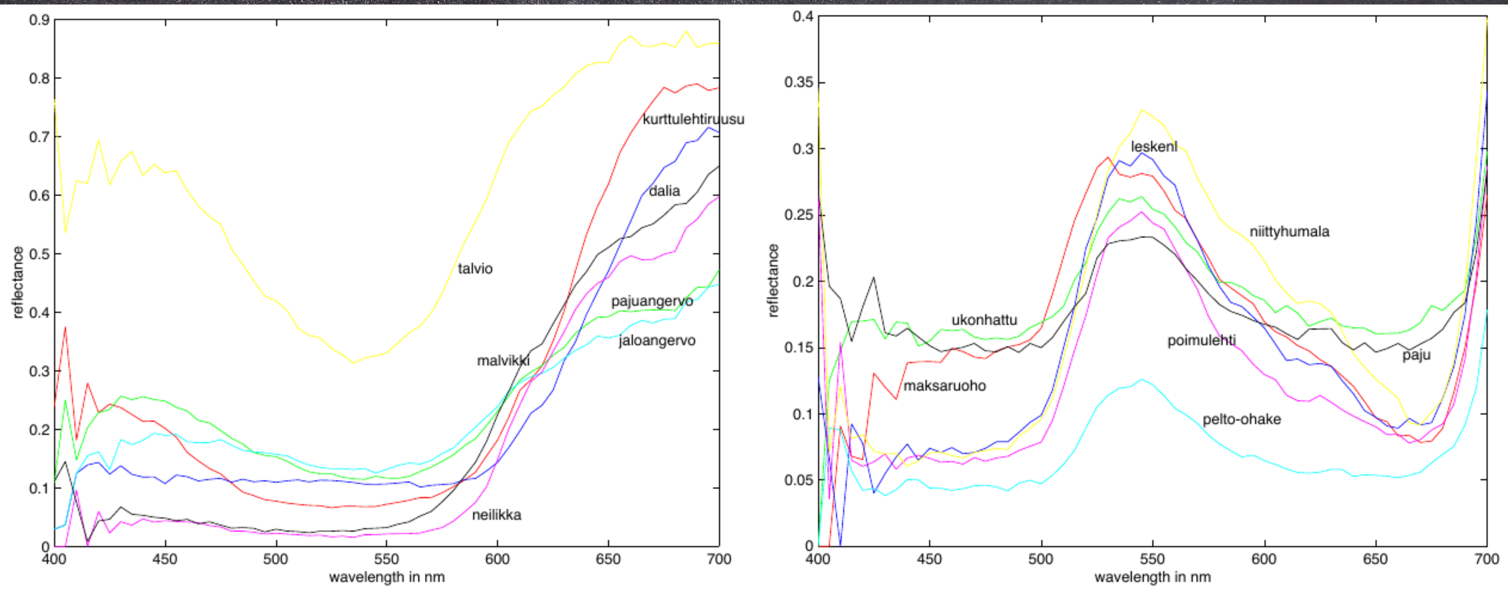

Figure 4.2. More spectral albedoes for a variety of natural surfaces, measured by Esa Koivisto, Department of Physics, University of Kuopio, Finland. On the left, albedoes for a series of different red flowers. Each is given its Finnish name. On the right, albedoes for green leaves; again, each is given its Finnish name. You should notice that these albedoes don't vary all that much. This is because there are relatively few mechanisms that give rise to colour in plants. These figures were plotted from data available at `http://www.it.lut.fi/research/color/lutcs_database.html`.

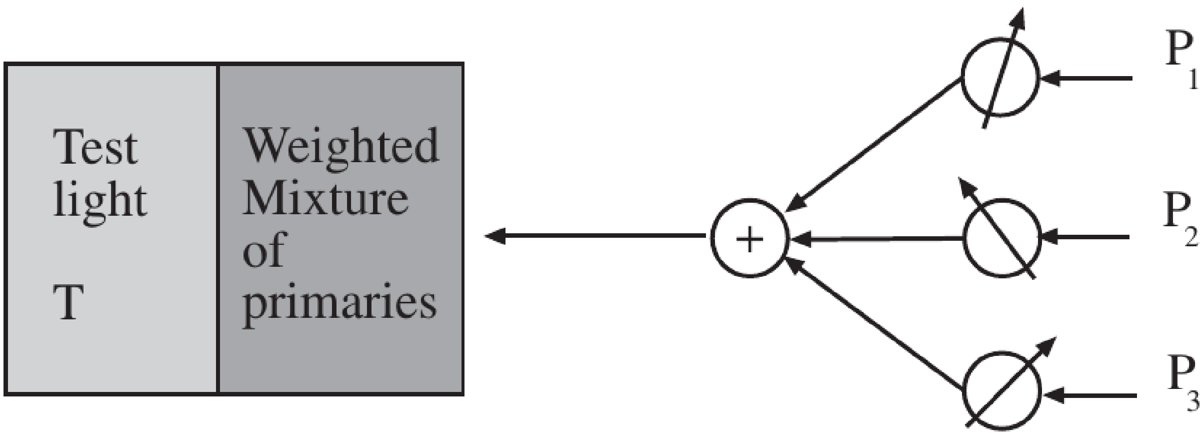

Figure 4.5. Human perception of colour can be studied by asking observers to mix coloured lights to match a test light, shown in a split field. The drawing shows the outline of such an experiment. The observer sees a test light T, and can adjust the amount of each of three primaries in a mixture that is displayed next to the test light. The observer is asked to adjust the amounts so that the mixture looks the same as the test light. The mixture of primaries can be written as $w_1P_1+w_2P_2+w_3P_3$; if the mixture matches the test light, then we write $T = w_1P_1 + w_2P_2 + w_3P_3$. It is a remarkable fact that for most people three primaries are sufficient to achieve a match for many colours, and for all colours if we allow subtractive matching (i.e. some amount of some of the primaries is mixed with the test light to achieve a match). Some people will require fewer primaries. Furthermore, most people will choose the same mixture weights to match a given test light.

Grassman 定律

$$
\begin{aligned}
T(\boldsymbol{w}) &= \sum_i w_i P_i \\
T(\boldsymbol{v}) &= \sum_i v_i P_i \\
T(k\boldsymbol{w}) + T(k\boldsymbol{v}) &= kT(\boldsymbol{w} + \boldsymbol{v})
\end{aligned}
$$

颜色感受体

$$p_k = \int_\Lambda \sigma_k(\lambda) E(\lambda) \mathrm{d}\lambda$$

彩色视觉

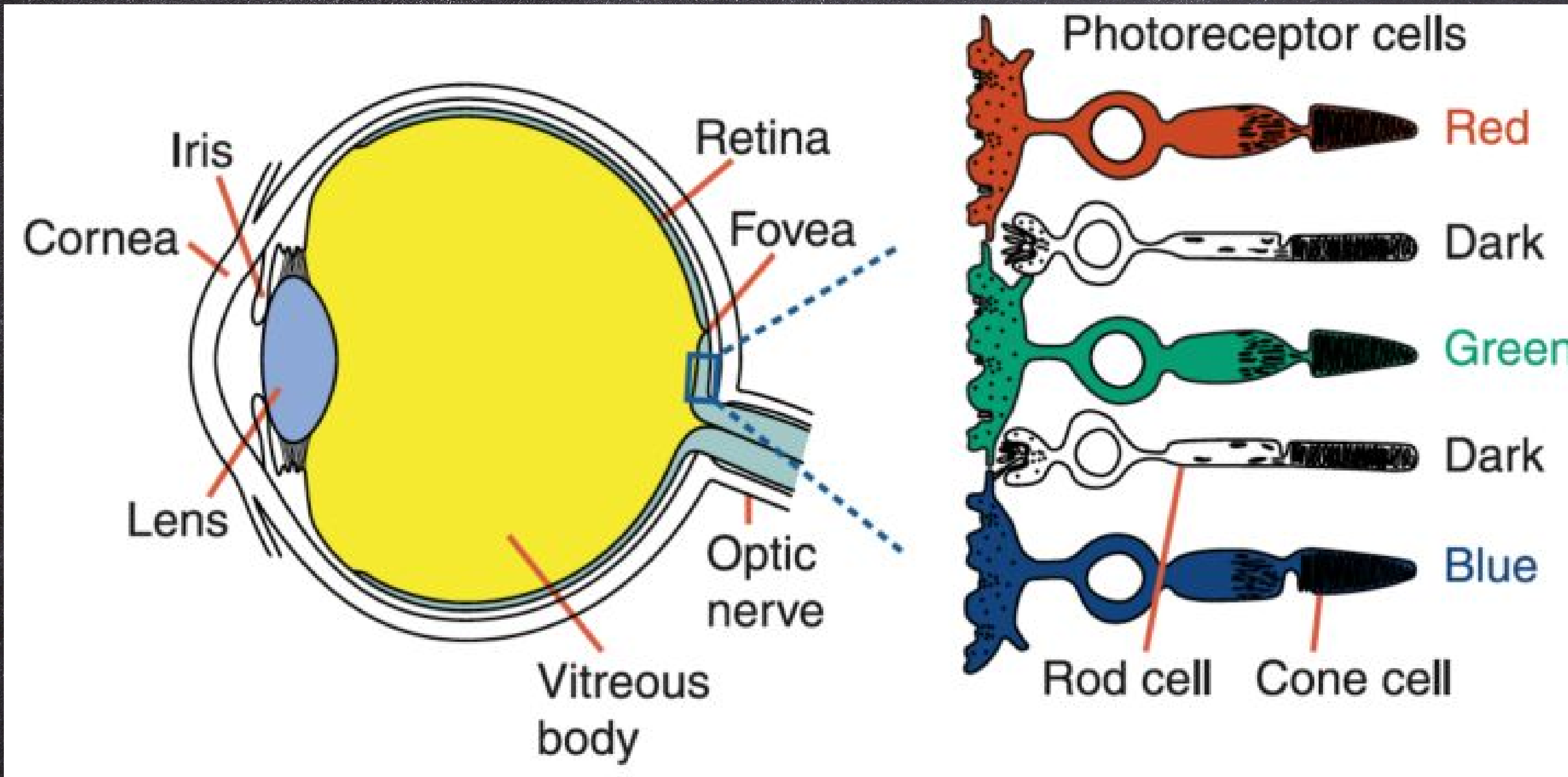
Photoreceptor cells
Iris
Retina
Cornea
Fovea
Lens
Optic
nerve
Vitreous
body
Red
Dark
Green
Dark
Blue
Rod cell
Cone cell

视锥细胞响应曲线

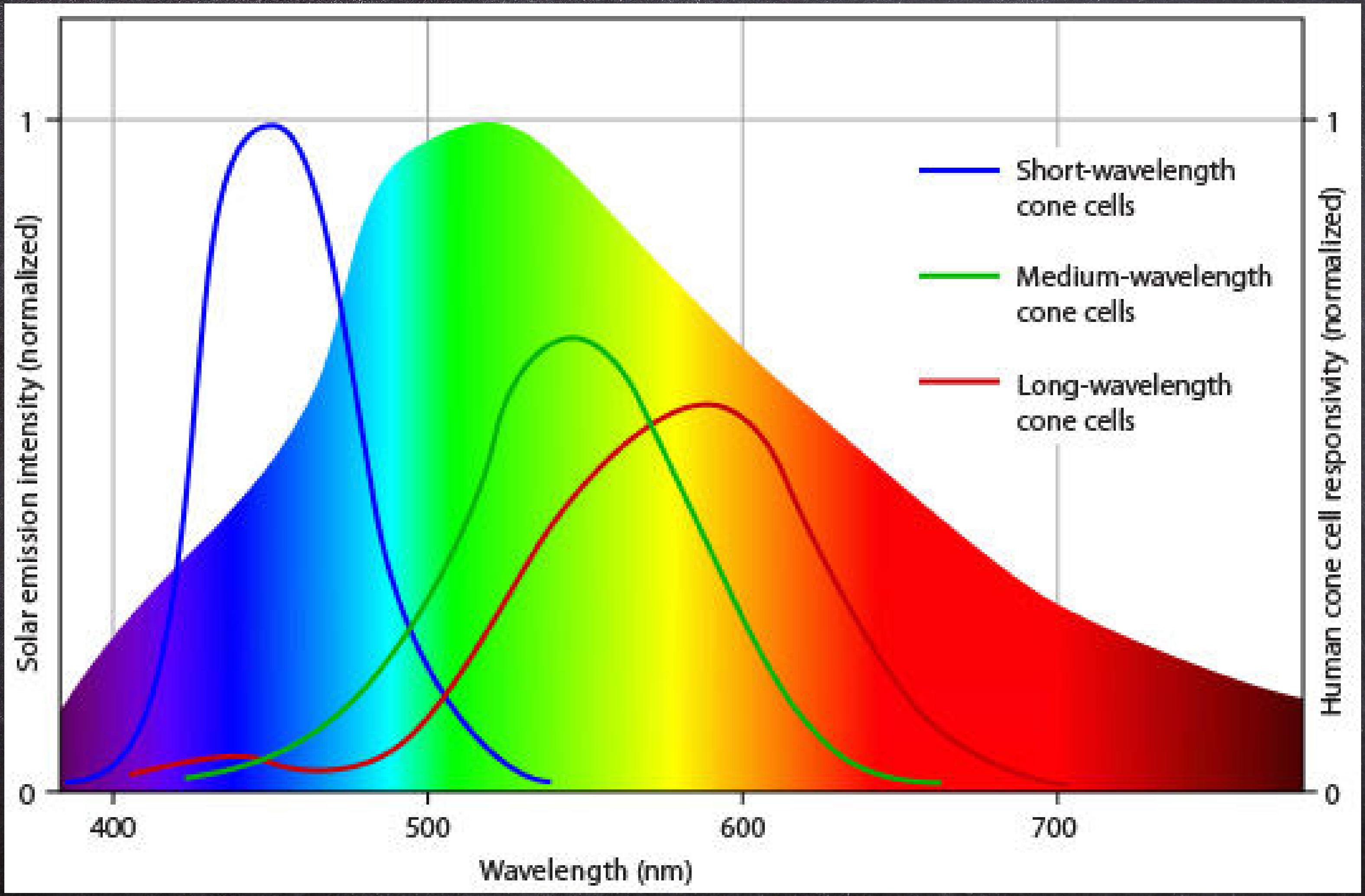
Short-wavelength cone cells
Medium-wavelength cone cells
Long-wavelength cone cells
Solar emission intensity (normalized)
Human cone cell responsivity (normalized)
Wavelength (nm)
400
500
600
700
0
1
0
1

颜色匹配函数

$$
\begin{aligned}
U(\lambda) &= f_1(\lambda)P_1 + f_2(\lambda)P_2 + f_3(\lambda)P_3 \\
S(\lambda) &= \left(\int_\Lambda f_1(\lambda)S(\lambda)\mathrm{d}\lambda\right)P_1 + \left(\int_\Lambda f_2(\lambda)S(\lambda)\mathrm{d}\lambda\right)P_2 + \left(\int_\Lambda f_3(\lambda)S(\lambda)\mathrm{d}\lambda\right)P_3
\end{aligned}
$$

线性颜色空间

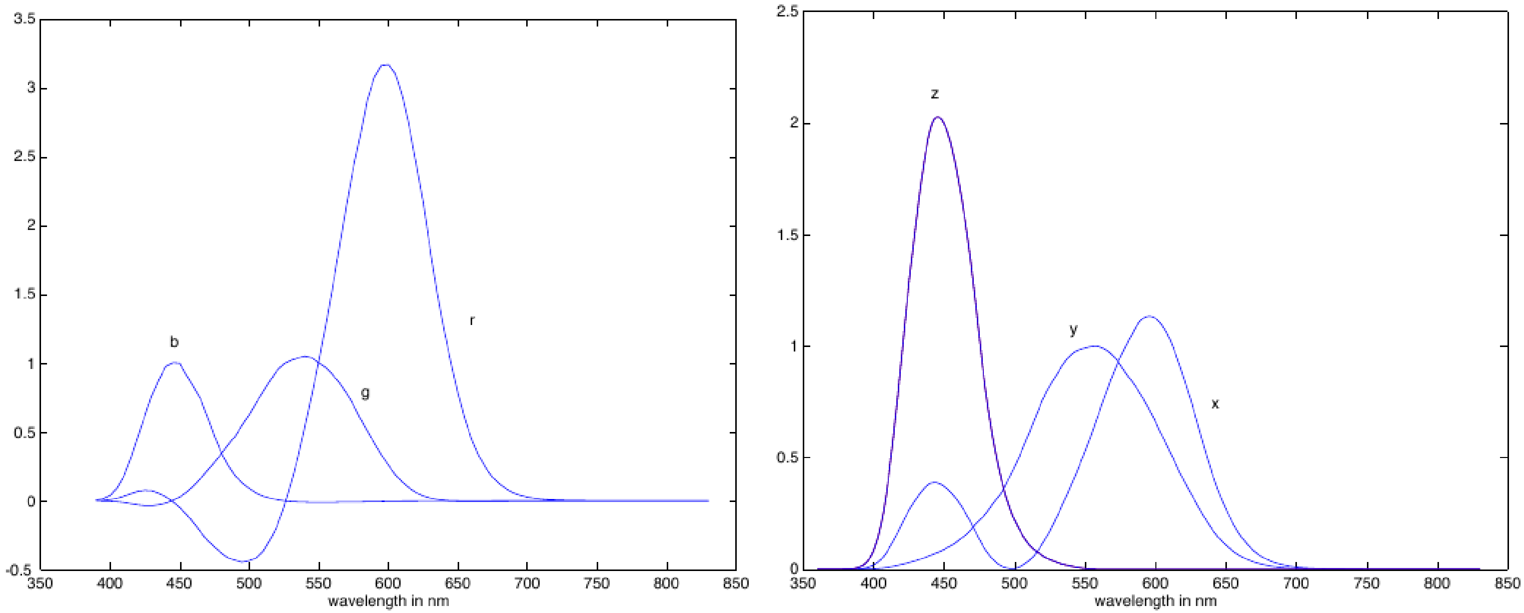

Figure 4.7. On the left, colour matching functions for the primaries for the RGB system. The negative values mean that subtractive matching is required to match lights at that wavelength with the RGB primaries. On the right, colour matching functions for the CIE X, Y and Z primaries; the colourmatching functions are everywhere positive, but the primaries are not real. Figures plotted from data available at `http://www-cvrl.ucsd.edu/index.htm`.

CIE XYZ颜色空间

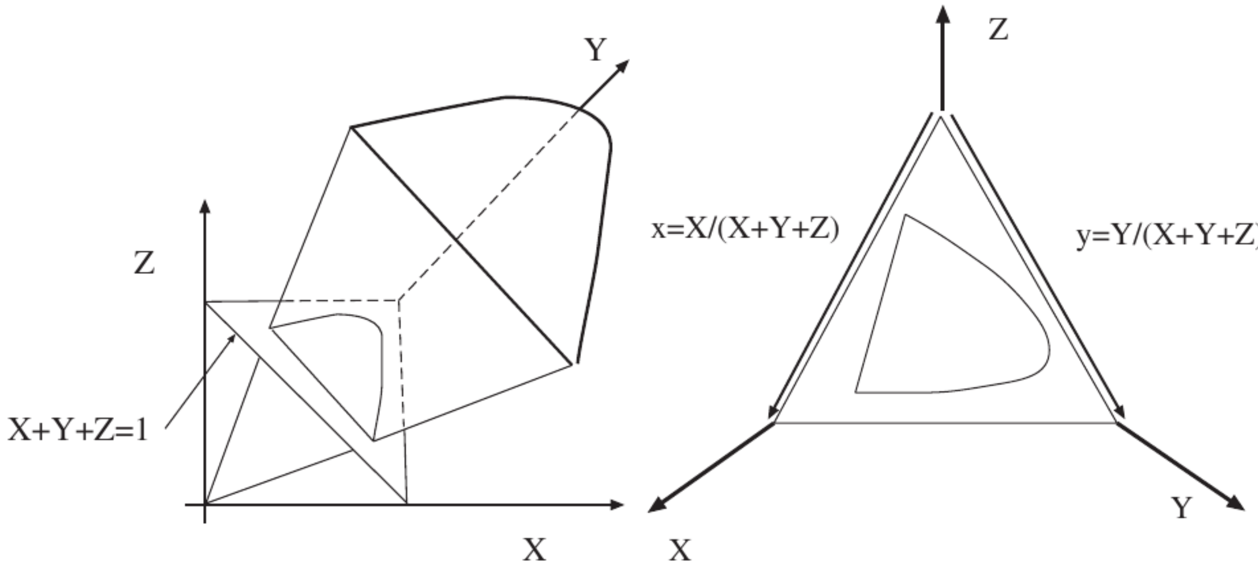

Figure 4.8. The volume of all visible colours in CIE XYZ coordinate space is a cone whose vertex is at the origin. Usually, it is easier to suppress the brightness of a colour — which we can do because to a good approximation perception of colour is linear — and we do this by intersecting the cone with the plane $X + Y + Z = 1$ to get the CIE xy space shown in figures 4.9 and 4.10

CIE xy

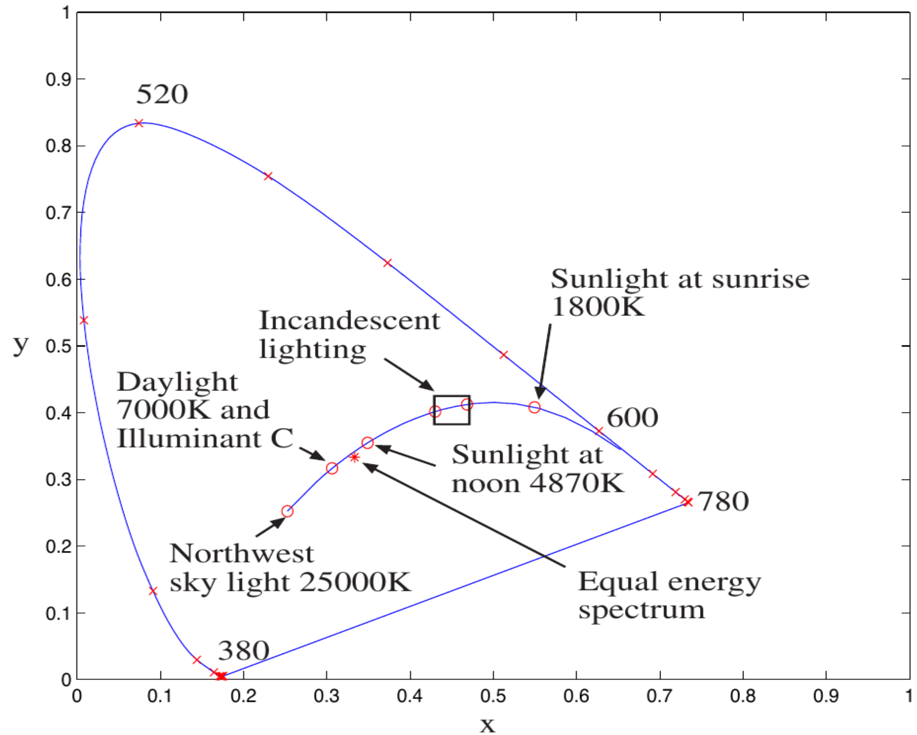

Figure 4.9. The figure shows a constant brightness section of the standard 1931 standard CIE xy colour space. This space has two coordinate axes. The curved boundary of the figure is often known as the spectral locus — it represents the colours experienced when lights of a single wavelength are viewed. The figure shows a locus of colours due to black-body radiators at different temperatures, and a locus of different sky colours. Near the center of the diagram is the neutral point, the colour whose weights are equal for all three primaries. CIE selected the primaries so that this light appears achromatic. Generally, colours that lie further away from the neutral point are more saturated — the difference between deep red and pale pink — and hue — the difference between green and red — as one moves around the neutral point.

Saturation & Hue

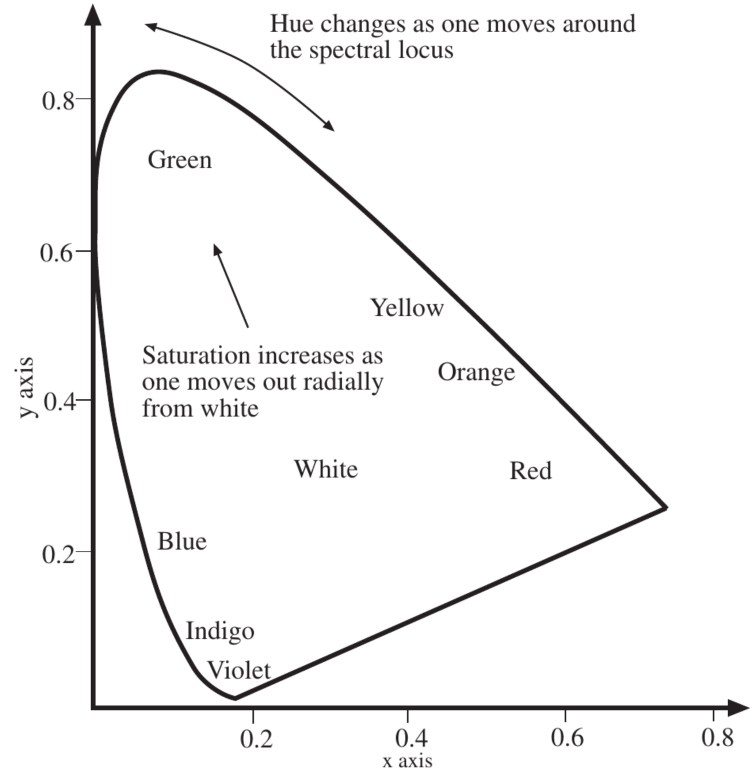

Figure 4.10. The figure shows a constant brightness section of the standard 1931 standard CIE xy colour space, with colour names marked on the diagram. Generally, colours that lie further away from the neutral point are more saturated — the difference between deep red and pale pink — and hue — the difference between green and red — as one moves around the neutral point.

颜色混合

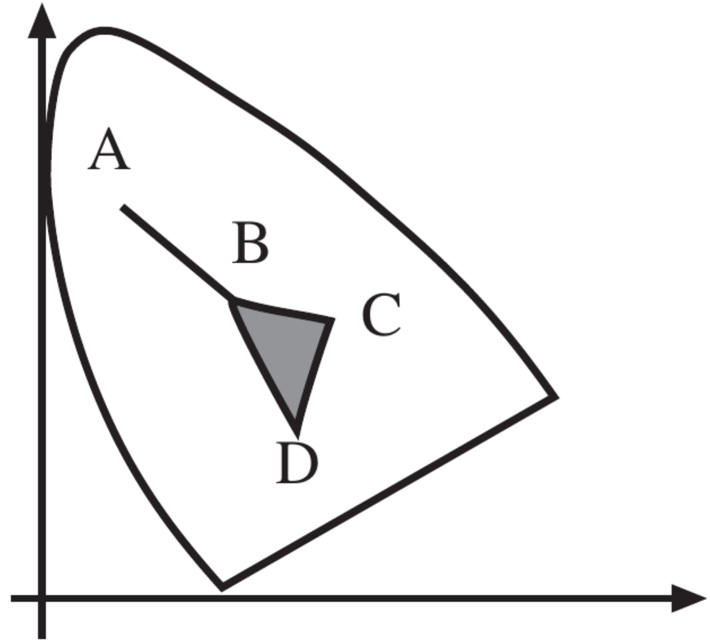

Figure 4.11. The linear model of the colour system allows a variety of useful constructions. If we have two lights whose CIE coordinates are $\boldsymbol{A}$ and $\boldsymbol{B}$ all the colours that can be obtained from non-negative mixtures of these lights are represented by the line segment joining $\boldsymbol{A}$ and $\boldsymbol{B}$. In turn, given $\boldsymbol{B}$, $\boldsymbol{C}$ and $\boldsymbol{D}$, the colours that can by obtained by mixing them lie in the triangle formed by the three points. This is important in the design of monitors — each monitor has only three phosphors, and the more saturated the colour of each phosphor the bigger the set of colours that can be displayed. This also explains why the same colours can look quite different on different monitors. The curvature of the spectral locus gives the reason that no set of three real primaries can display all colours without subtractive matching.

RGB颜色空间

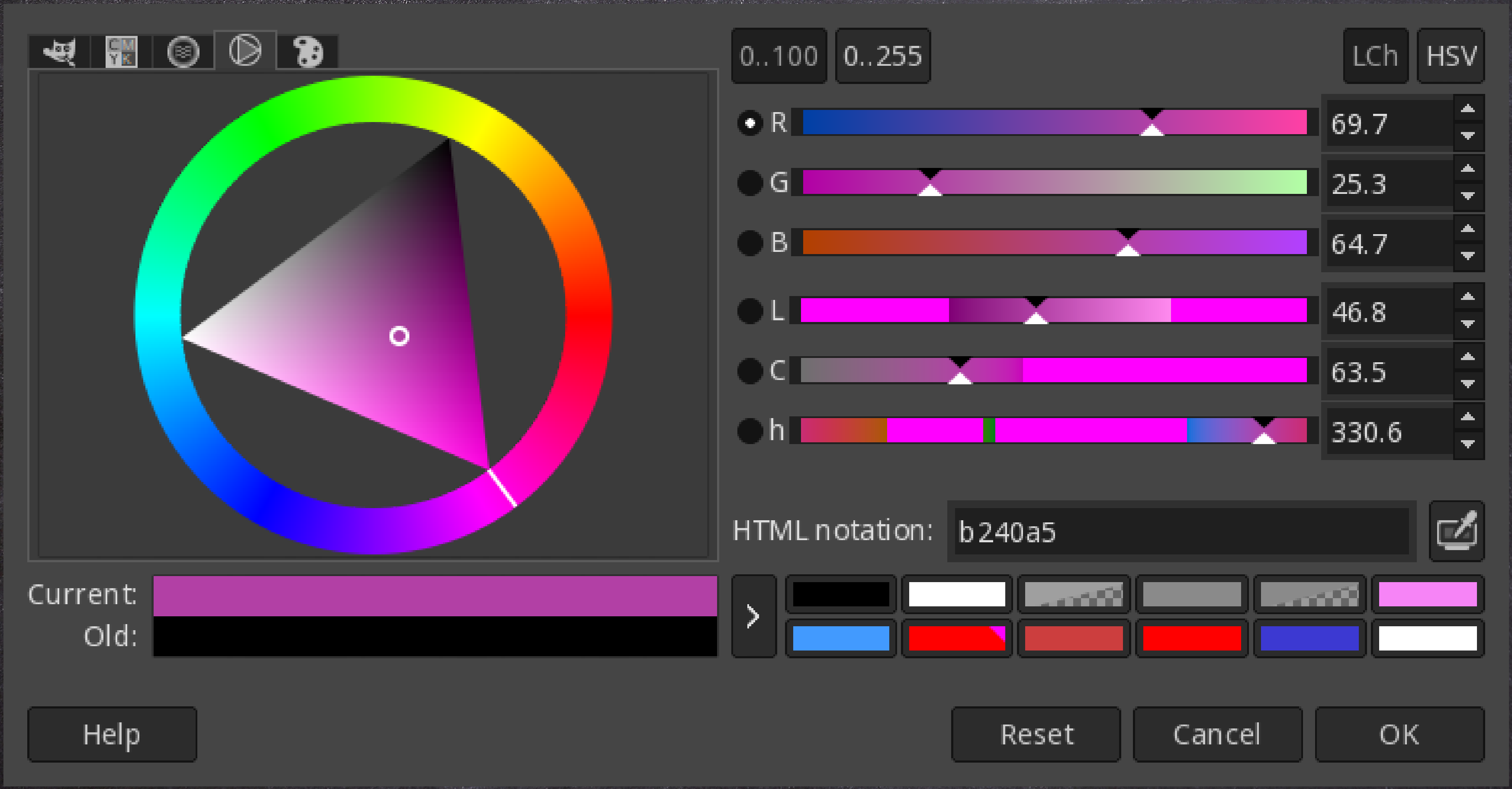
0..100
0..255
LCh
HSV
R
69.7
G
25.3
B
64.7
L
46.8
C
63.5
h
330.6
HTML notation:
b240a5
Current:
Old:
Help
Reset
Cancel
OK

CMYK颜色空间

- cyan (a blue-green colour) = W – R (white – red);
- magenta (a purplish colour) = W – G (white – green)
- and yellow = W – B (white – blue)

Hue, Saturation and Value

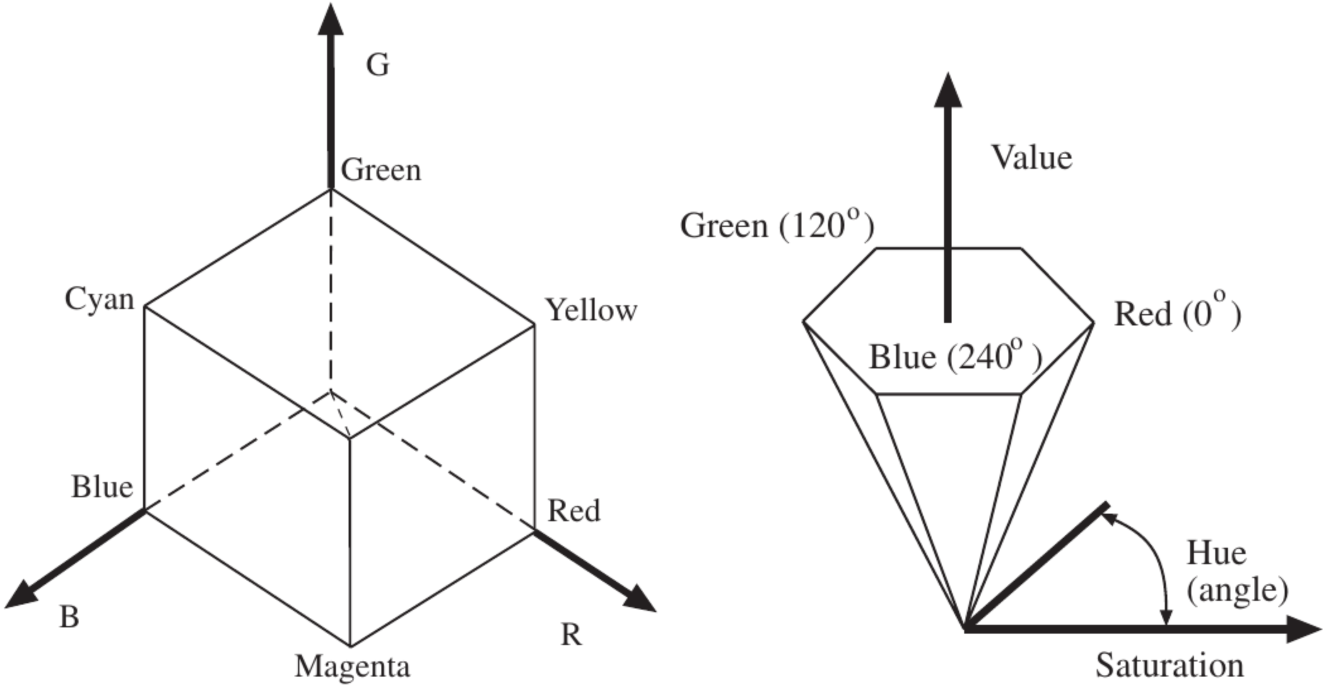

Figure 4.12. On the left, we see the RGB cube; this is the space of all colours that can be obtained by combining three primaries (R, G, and B — usually defined by the colour response of a monitor) with weights between zero and one. It is common to view this cube along its neutral axis — the axis from the origin to the point (1, 1, 1) — to see a hexagon, shown in the middle. This hexagon codes hue (the property that changes as a colour is changed from green to red) as an angle, which is intuitively satisfying. On the right, we see a cone obtained from this cross-section, where the distance along a generator of the cone gives the value (or brightness) of the colour, angle around the cone gives the hue and distance out gives the saturation of the colour.

均匀颜色空间

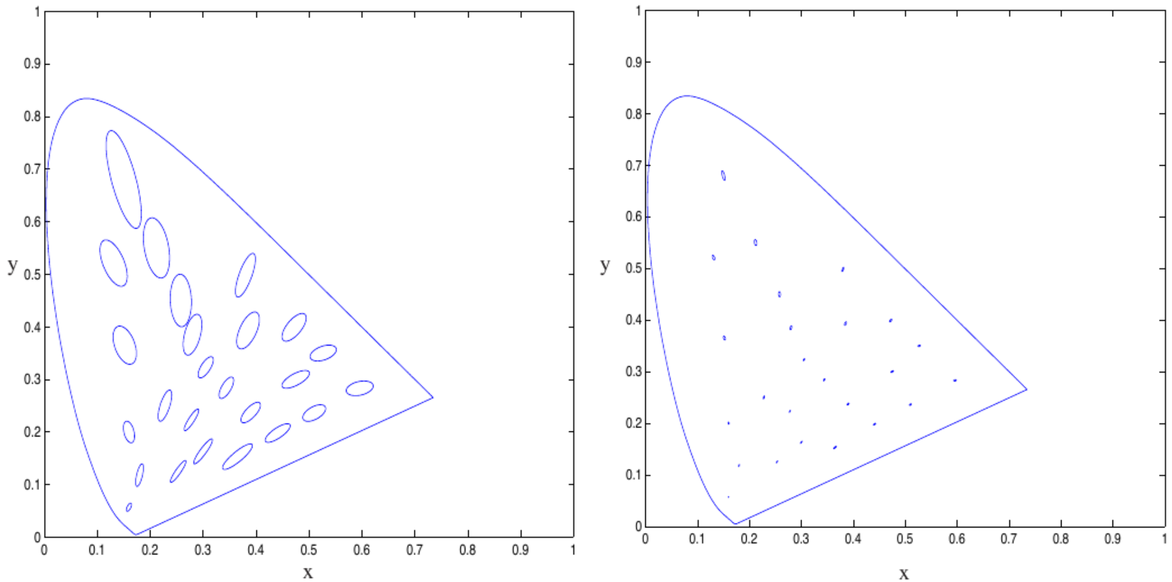

Figure 4.13. This figure shows variations in colour matches on a CIE x, y space. At the center of the ellipse is the colour of a test light; the size of the ellipse represents the scatter of lights that the human observers tested would match to the test colour; the boundary shows where the just noticeable difference is. The ellipses in the figure on the **left** have been magnified 10x for clarity, and on the **right** they are plotted to scale. The ellipses are known as MacAdam ellipses, after their inventor. Notice that the ellipses at the top are larger than those at the bottom of the figure, and that they rotate as they move up. This means that the magnitude of the difference in x, y coordinates is a poor guide to the difference in colour. Ellipses plotted using data from Macadam's paper of 1942 [MacAdam, 1942].

CIE u'v'颜色空间

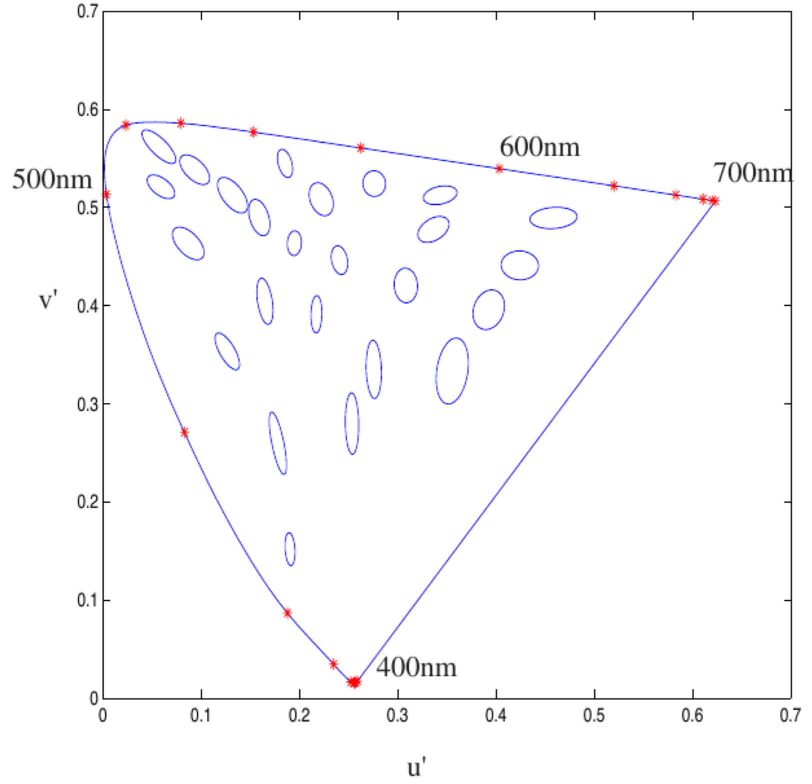

Figure 4.14. This figure shows the CIE 1976 u', v' space, which is obtained by a projective transformation of CIE x, y space. The intention is to make the MacAdam ellipses uniformly circles — this would yield a uniform colour space. A variety of non-linear transforms can be used to make the space more uniform (see [Fairchild, 1998] for details)

CIE LAB颜色空间

$$
\begin{aligned}
L^* &= 116\left(\frac{Y}{Y_n}\right)^{\frac{1}{3}} - 16 \\
a^* &= 500\left(\left(\frac{X}{X_n}\right)^{\frac{1}{3}} - \left(\frac{Y}{Y_n}\right)^{\frac{1}{3}}\right) \\
b^* &= 200\left(\left(\frac{Y}{Y_n}\right)^{\frac{1}{3}} - \left(\frac{Z}{Z_n}\right)^{\frac{1}{3}}\right)
\end{aligned}
$$

图像颜色模型

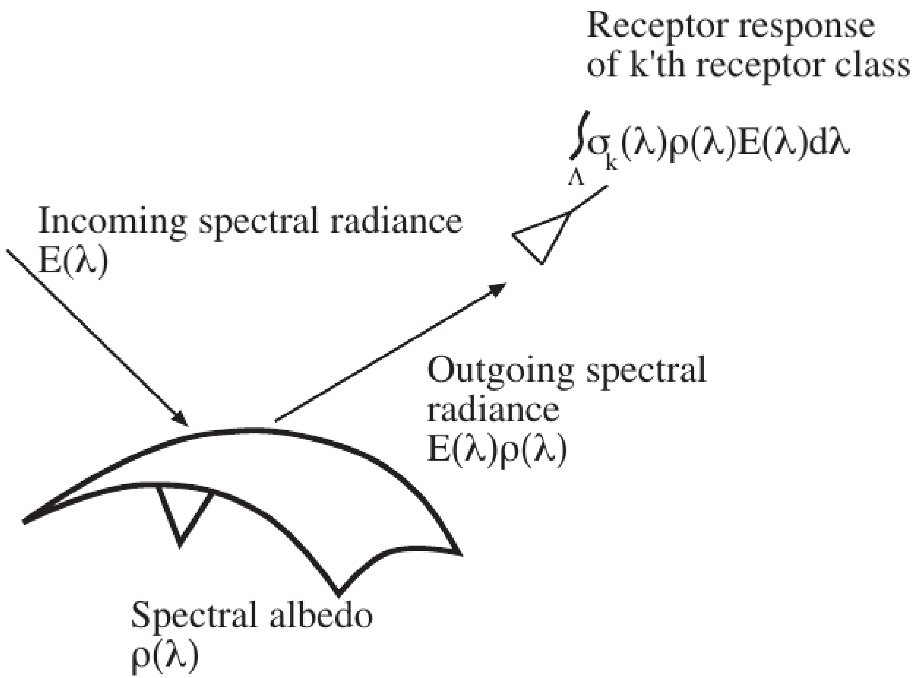

Figure 4.15. If a patch of perfectly diffuse surface with diffuse spectral reflectance $\rho(\lambda)$ is illuminated by a light whose spectrum is $E(\lambda)$, the spectrum of the reflected light will be $\rho(\lambda)E(\lambda)$ (multiplied by some constant to do with surface orientation, which we have already decided to ignore). Thus, if a linear photoreceptor of the k'th type sees this surface patch, its response will be: $p_k = \int_\Lambda \sigma_k(\lambda)\rho(\lambda)E(\lambda)d\lambda$ where Λ is the range of all relevant wavelengths and $\sigma_k(\lambda)$ is the sensitivity of the k'th photoreceptor.

$$\begin{aligned}\boldsymbol{C}(\boldsymbol{x}) &= \text{(diffuse term)} + \text{(specular term)} \\ &= \text{(direct term)} + \text{(interreflected term)} + \text{(specular term)} \\ &= g_d(\boldsymbol{x})\boldsymbol{d}(\boldsymbol{x}) + \boldsymbol{i}(\boldsymbol{x}) + g_s(\boldsymbol{x})\boldsymbol{s}(\boldsymbol{x})\end{aligned}$$

$\boldsymbol{d}(\boldsymbol{x})$模型：

$$p_k = \int_\Lambda \sigma_k(\lambda)\rho(\lambda)S(\lambda)\mathrm{d}\lambda$$

漫反射与镜面反射

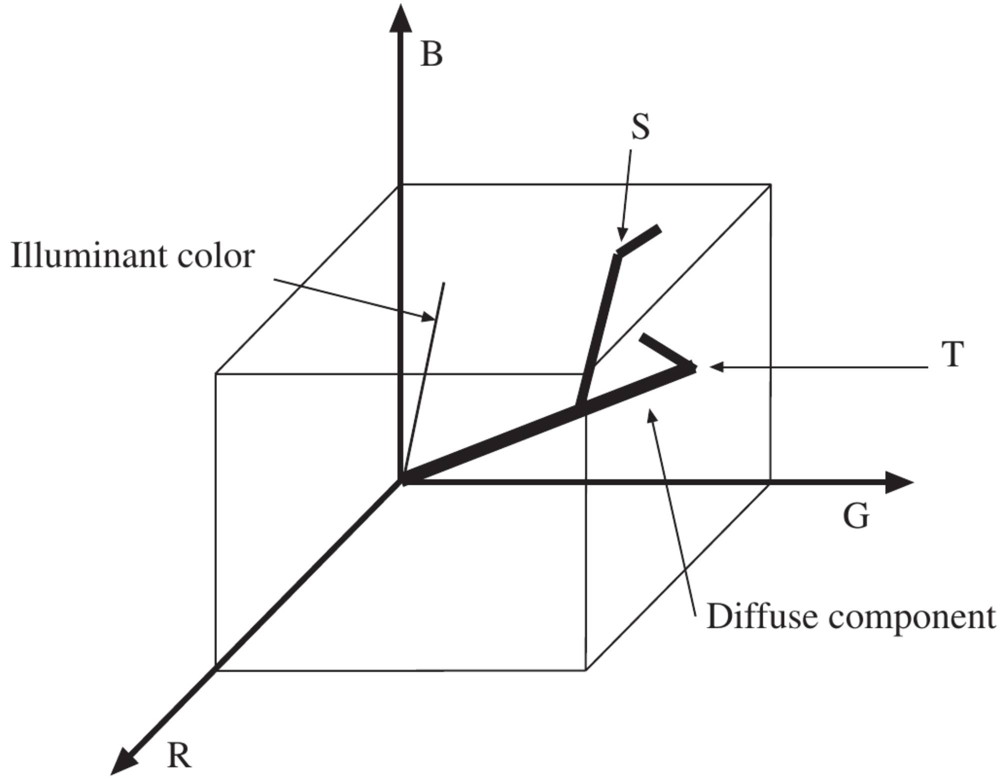

Figure 4.20. Assume we have a picture of a single uniformly coloured surface. Our model of reflected light should lead to a gamut that looks like the drawing. We are assuming that reflected light consists of the diffuse term plus a specular term, and the specular term is the colour of the light source. Most points on the surface do not have a significant specular term, and instead are brighter or darker versions of the same diffuse surface colour. At some points, the specular term is large, and this leads to a "dog-leg" in the gamut, caused by adding the diffuse term to the source term. If the diffuse reflection is very bright, one or another colour channel might saturate (point T); similarly, if the specular reflection is very bright one or another colour channel might saturate (point "S").

找到镜面反射

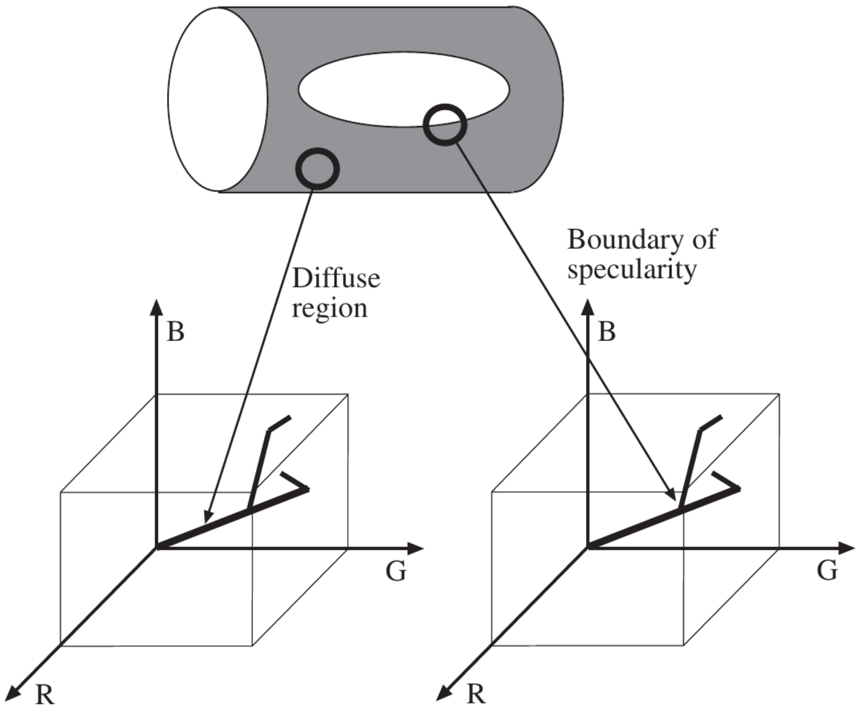

Figure 4.21. The linear clusters produced by specularities on plastic objects can be found by reasoning about windows of image pixels. In a world of plastic objects on a black background, a background window produces a region of pixels that are point-like in colour space — all pixels have the same colour. A window that lies along the body produces a line-like cluster of points in colour space, because the intensity varies but the colour does not. At the boundary of a specularity, windows produce plane-like clusters, because points are a weighted combination of two different colours (the specular and the body colour). Finally, at interior of a specular region, the windows can produce volume-like clusters, because the camera saturates, and the extent of the window can include both the boundary style window points and the saturated points. Whether a region is line-like, plane-like or volume like can be determined easily by looking at the eigenvalues of the covariance of the pixels.

阴影消除

$$
\begin{aligned}
E(\lambda;T) &= K\lambda^{-5}e^{\frac{-hc}{k\lambda T}} \\
\sigma_k(\lambda) &= \delta(\lambda-\lambda_k) \\
r_j &= \int \sigma_j(\lambda)\rho(\lambda)K\lambda^{-5}e^{\frac{-hc}{k\lambda T}}\mathrm{d}\lambda \\
&= K\rho(\lambda)\lambda_j^{-5}e^{\frac{-hc}{k\lambda_j T}}
\end{aligned}
$$

颜色空间

$$
\begin{aligned}
c_1 &= \log\left(\frac{r_1}{r_3}\right) \\
c_2 &= \log\left(\frac{r_2}{r_3}\right) \\
\begin{pmatrix} c_1 \\ c_2 \end{pmatrix} &= \begin{pmatrix} a_1 \\ a_2 \end{pmatrix} + \frac{1}{T}\begin{pmatrix} b_1 \\ b_2 \end{pmatrix}
\end{aligned}
$$

颜色方向

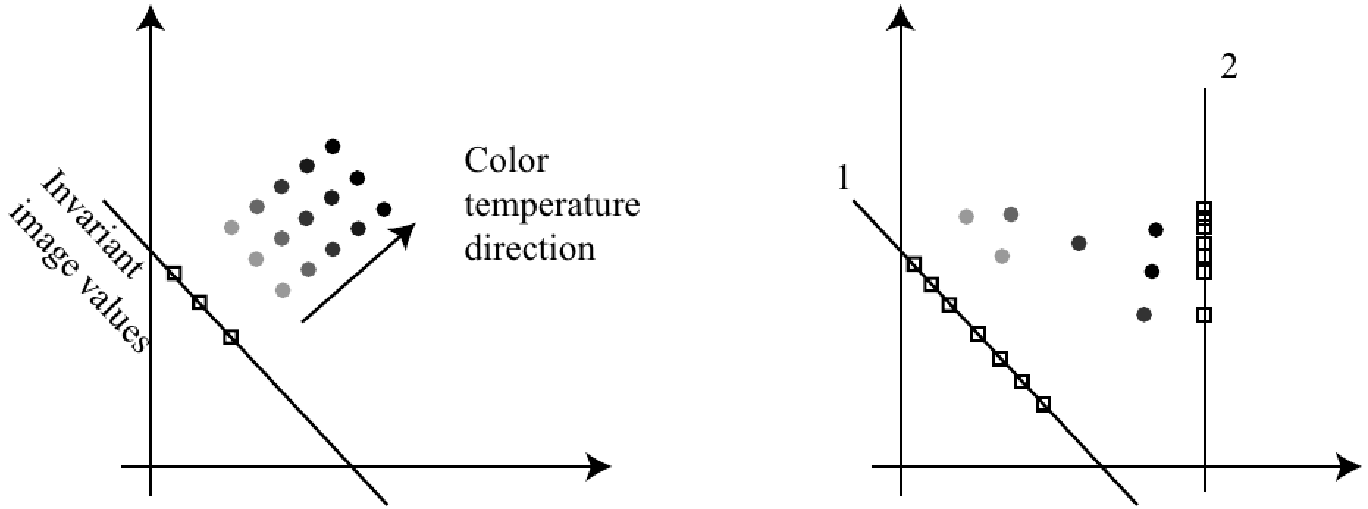

FIGURE 3.19: Changing the color temperature of the light under which a surface is viewed moves the (c_1, c_2) coordinates of that surface along the color temperature direction (**left**; the different gray patches represent the same surface under different lights). If we now project the coordinates along the (c_1, c_2) direction onto some line, we obtain a value that doesn't change when the illuminant color temperature changes. This is the invariant value for that pixel. Generally, we do not know enough about the imaging system to estimate the color temperature direction. However, we expect to see many different surfaces in each scene; this suggests that the right choice of color temperature direction on the **right** is 1 (where there are many different types of surface) rather than 2 (where the range of invariant values is small).

颜色恒常性

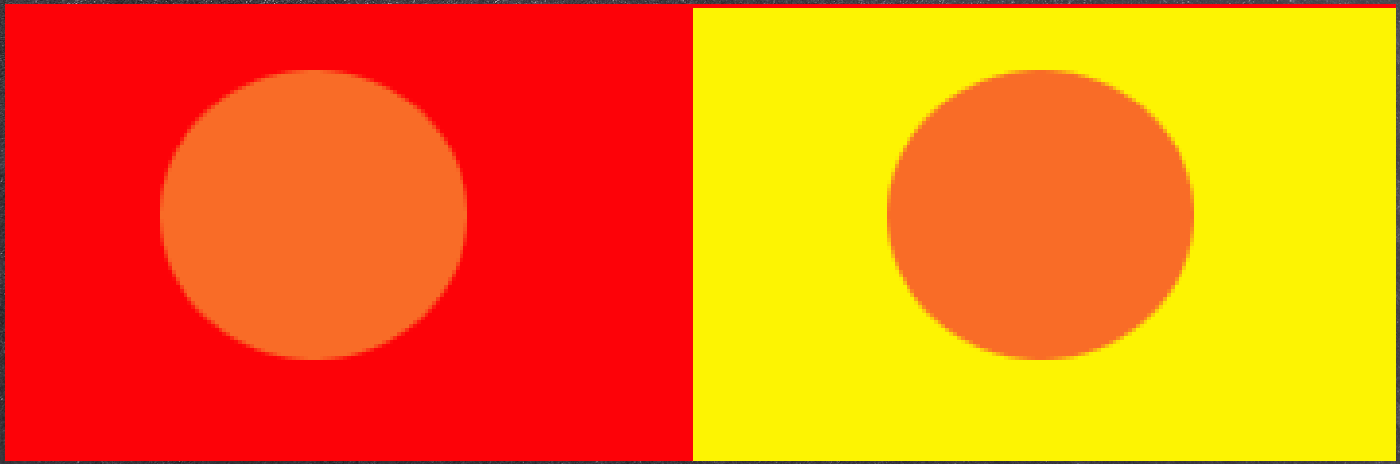

有限维线性模型

$$
\begin{aligned}
\rho(\lambda) &= \sum_{j=1}^{n} r_j \varphi_j(\lambda) \\
E(\lambda) &= \sum_{i=1}^{m} e_i \psi_i(\lambda) \\
p_k &= \int \sigma_k(\lambda) \left(\sum_{j=1}^{n} r_j \varphi_j(\lambda) \right) \left(\sum_{i=1}^{m} e_i \psi_i(\lambda) \right) \mathrm{d}\lambda \\
&= \sum_{j=1}^{n} \sum_{i=1}^{m} e_i r_j \int \sigma_k(\lambda) \varphi_j(\lambda) \psi_i(\lambda) \mathrm{d}\lambda \\
&= \sum_{j=1}^{n} \sum_{i=1}^{m} e_i r_j g_{ijk}
\end{aligned}
$$

推断表面颜色（镜面反射率相同）

已知σ_k, ψ_i求e_i:

$$
\begin{aligned}
p_k &= \int \sigma_k(\lambda) \sum_{i=1}^{m} e_i \psi_i(\lambda) \mathrm{d}\lambda \\
&= \sum_{i=1}^{m} \sum_{j=1}^{n} \int \sigma_k(\lambda) e_i \psi_i(\lambda) \mathrm{d}\lambda
\end{aligned}
$$

r_j:

$$
p_k = \sum_{j=1}^{n} \sum_{i=1}^{m} e_i r_j g_{ijk}
$$

推断表面颜色（平均反射率是常数）

已知$\bar{p}_k, \bar{r}_j$,求e_i

$$\begin{aligned}
\bar{\rho} &= \sum_{j=1}^{n} \bar{r}_j \varphi_j(\lambda) \\
\bar{p}_k &= \sum_{j=1}^{n} \sum_{i=1}^{m} e_i g_{ijk} \bar{r}_j
\end{aligned}$$

r_j:

$$p_k = \sum_{j=1}^{n} \sum_{i=1}^{m} e_i r_j g_{ijk}$$